Neurotherapeutics
https://doi.org/10.1007/s13311-018-0613-8

ORIGINAL ARTICLE

Brain Renin–Angiotensin System Blockade Attenuates Methamphetamine-Induced Hyperlocomotion and Neurotoxicity

Linhong Jiang[1] · Ruiming Zhu[1] · Qian Bu[1,2] · Yan Li[1] · Xue Shao[1] · Hui Gu[1] · Jueying Kong[1] · Li Luo[1] · Hailei Long[1] · Wei Guo[1,3,4] · Jingwei Tian[3,4] · Yinglan Zhao[1] · Xiaobo Cen[1]

Abstract

Methamphetamine (METH) abuse has become a major public health concern worldwide without approved pharmacotherapies. The brain renin–angiotensin system (RAS) is involved in the regulation of neuronal function as well as neurological disorders. Angiotensin II (Ang II), which interacts with Ang II type 1 receptor (AT_1-R) in the brain, plays an important role as a neuromodulator in dopaminergic transmission. However, the role of brain RAS in METH-induced behavior is largely unknown. Here, we revealed that repeated METH administration significantly upregulated the expression of AT_1-R in the striatum of mice, but downregulated dopamine D3 receptor (D3R) expression. A specific AT_1-R blocker telmisartan, which can penetrate the brain–blood barrier (BBB), or genetic deletion of AT_1-R was sufficient to attenuate METH-triggered hyperlocomotion in mice. However, intraperitoneal injection of AT_1-R blocker losartan, which cannot penetrate BBB, failed to attenuate METH-induced behavior. Moreover, intra-striatum re-expression of AT_1 with lentiviral virus expressing AT_1 reversed the weakened locomotor activity of $AT_1^{-/-}$ mice treated with METH. Losartan alleviated METH-induced cytotoxicity in SH-SY5Y cells *in vitro*, which was accompanied by upregulated expressions of D3R and dopamine transporter. In addition, intraperitoneal injection of perindopril, which is a specific ACE inhibitor and can penetrate BBB, significantly attenuated METH-induced hyperlocomotor activity. Collectively, our results show that blockade of brain RAS attenuates METH-induced hyperlocomotion and neurotoxicity possibly through modulation of D3R expression. Our findings reveal a novel role of Ang II–AT_1-R in METH-induced hyperlocomotion.

Keywords AT_1-R · Methamphetamine · Angiotensin II · D3R · Hyperlocomotion · Neurotoxicity.

Linhong Jiang and Ruiming Zhu contributed equally to this work.

Electronic supplementary material The online version of this article (https://doi.org/10.1007/s13311-018-0613-8) contains supplementary material, which is available to authorized users.

✉ Xiaobo Cen
xbcen@scu.edu.cn

[1] National Chengdu Center for Safety Evaluation of Drugs, State Key Laboratory of Biotherapy and Cancer Center, West China Hospital, Sichuan University, and Collaborative Innovation Center for Biotherapy, #1 Keyuan Road 4, Gaopeng Street, High-tech Development Zone, Chengdu 610041, China

[2] Department of Food Science and Technology, College of Light Industry, Textile and Food Engineering, Sichuan University, Chengdu 610065, China

[3] School of Pharmacy, Yantai University, Yantai 264003, China

[4] State Key Laboratory of Long-Acting and Targeting Drug Delivery Technologies, Yantai 264003, China

Introduction

Methamphetamine (METH), a highly addictive psychostimulant, has become a major worldwide public health concern [1]. Repeated administration of METH induces psychostimulant behaviors and causes neurotoxicity in the striatum by increasing extracellular dopamine (DA) concentration through facilitating DA release and/or inhibiting its reuptake [2, 3]. Studies have shown that METH-induced hyperlocomotion and neurotoxicity are associated with an increase in dopaminergic transmission in the brain, which is mediated by the structural plasticity of dopaminergic mesolimbic system [2]. Dopamine D3 receptor (D3R), a member of the D2-like DA receptor family, has emerged as a compelling therapeutic target for addictions and related disorders [4–7]. Exposure to METH induces alterations in locomotor activity and cognitive function by impairing dopaminergic function in the

Published online: 20 February 2018

striatum [8]. Moreover, a negative association between impulsivity and striatal D3R expression is observed in METH users [9, 10].

The renin–angiotensin system (RAS) is a hormone system that is involved in the regulation of the plasma sodium concentration and arterial blood pressure. It is now well established that the brain has its own intrinsic RAS with all its components, such as Ang II, angiotensin-converting enzyme (ACE), and AT_1-R [11]. Brain RAS is involved in the regulation of neuronal function as well as brain diseases, such as Alzheimer's and Parkinson's diseases [12–14]. Ang II is thought to be a modulator of DA release and plays an important role in the regulation of central dopaminergic neurotransmission [15]. Ang II type 1 and 2 receptors (AT_1-R and AT_2-R) are expressed in the mesolimbic dopaminergic neurons, and Ang II facilitates dopamine release in the striatum through interaction with AT_1-R both *in vitro* and *in vivo* [16]. Moreover, AT_1-R is highly expressed in DA-rich brain areas [17, 18]. AT_1-R antagonist increases dopamine D1 receptor (D1R) but decreases D3R expression [19, 20]. AT_1-R interacts with D2R directly, forming functional heteromers in the striatal neurons [21]. Studies suggest that interaction between AT_1-R and amphetamine (AMPH) participates in the neuroadaptative and long-term changes in AT_1-R density as well as angiotensinogen expression [22, 23]. Increased locomotor activity induced by AMPH challenge is inhibited by AT_1-R antagonist losartan administration in the caudate putamen of rats [24]. AT_1-R is also involved in learning and memory alterations induced by amphetamine in rats [25]. These findings hint the potential role of brain RAS components in neuroadaptative changes. However, the role of brain RAS in METH-induced behavioral effect is largely unknown.

In the present study, we demonstrated that pharmacological blockade or genetic knockout of AT_1-R attenuates METH-triggered hyperlocomotion in mice. AT_1-R participates in METH-induced behavioral effect possibly through negative modulation of D3R expression.

Materials and Methods

Drugs

METH-HCl was purchased from the National Institute for the Control of Pharmaceutical and Biological Products (Beijing, China). METH was dissolved in 0.9% saline. Perindopril erbumine, telmisartan, and losartan potassium were purchased from Selleck Chemicals (Houston, TX).

Animals

Adults male C57BL/6 mice (8-12 weeks old, body weight 22-24 g) were bred and housed in clear plastic cages with 12 h light/dark cycle (07:00/19:00 h) at constant temperature (20-25 °C) with food and water ad libitum. Before behavioral testing began, the mice were adapted to the conditions for 3 days. All experimental procedures and use of the animals were in accordance with the study protocols which were approved by the Institutional Animal Care and Use Committee of Sichuan University. $AT_1^{-/-}$ mice with C57BL/6 background were purchased from The Jackson Laboratory (No. 002682). Gene identification of mice was conducted, and the mice with AT_1 knockout homozygote were used. The whole genes were obtained from mice tails and amplified with polymerase chain reaction (PCR). Different genes were separated and distinguished by agarose gel electrophoresis.

Construction of Lentiviral Vectors Plasmids for Expressing AT_1-R

EX-Mm01127-LV201 and EX-NEG-LV201 virus plasmids were constructed for the production of lentivirus expressing AT_1 and green fluorescent protein (GFP) (LV-AT_1) as well as lentivirus expressing GFP (LV-GFP) only. The plasmid design and construction of LV-AT_1 and LV-GFP are shown in Supplementary Fig. S1. The lentivirus was packaged by viral packaging system (GeneCopoeia, China) in 293T cells. Viral titers were determined by infection of 293T cells and GFP visualization (4.94 × 108 TU/ml). The results revealed that LV-AT_1 upregulated AT_1-R mRNA specifically in $AT_1^{-/-}$ mice (Supplementary Fig. S2). The sequence of LV-AT_1 is shown in Supplementary Table S1.

Intra-striatum Injection of Lentivirus

Under 10% chloralhydrate anesthesia (0.1 ml per mice), mice were fixed on the stereotaxic apparatus, and the cranium surface was exposed. By using a microinjector, 2 μl lentivirus was bilaterally infused into the striatum at a 90° angle (anteroposterior, + 1.0; mediolateral, ± 2.0; dorsoventral, − 2.9) at a rate of 0.1 μl/min. After injection, syringe needles were maintained in the striatum for 1 min. Animals receiving the lentivirus injection were recovered for a week until the beginning of the tests.

Drug Injection

Repeated METH Treatment

Mice were intraperitoneally (i.p.) injected with 1 mg/kg METH daily for 7 days continuously. For investigating the time-dependent expression of AT_1-R in response to METH, mice were euthanized at 1, 2, 3, 5, and 7 days after the last METH injection, respectively.

Inhibitor Treatment

The ACE inhibitor (perindopril) and AT_1-R inhibitors (losartan or telmisartan) were used to treat the mice, respectively. Perindopril (0.5 mg/kg), losartan (5 mg/kg), or telmisartan (5 mg/kg) was injected intraperitoneally into the mice 30 min before METH administration.

METH-Induced Hyperlocomotion

The apparatus and protocol of locomotor activity test have been described in a previous study [26]. Briefly, each mouse was evaluated in the acrylic chambers (40.64 × 40.64 × 31 cm) with black plastic walls. This apparatus was equipped with a camera directly above the cross of four separated chambers. This camera recorded each mouse's movement distance and routes. EthoVision version 7.0 software (Noldus Information Technology, Netherlands) was used for automate tracking. Each of the mice was placed in the chamber after intraperitoneal injection of 1 mg/kg METH or 0.9% saline. Behavior sessions were conducted daily for 7 days continuously, and every session lasted 15 min per day.

Tissue Isolation

At the end of the testing session, mice were euthanized, and brains were rapidly collected. The striatum, nucleus accumbens (NAc), prefrontal cortex (PFC), and hippocampus were isolated immediately, frozen in liquid nitrogen, and then stored at − 80 °C for further processing.

RNA Isolation and Quantitative Reverse Transcription-PCR Detection

Bilateral striatum samples were homogenized in TRIzol, and then processed according to the instructions. The purified RNA was determined by agarose gel electrophoresis following protocol, then spectroscopy confirmed the concentration of RNA by Image Lab. The purified RNA was reversed using DBI Bioscience Kit (Germany). The cDNA was quantified by quantitative reverse transcription-PCR (qRT-PCR) using SYBR Green. Every reaction was run 3 times and analyzed with the $2^{-\Delta\Delta Ct}$ method. All primer sequences are listed in Supplementary Table S2.

Western Blot Analysis

Western blot analysis was performed as previously described [26]. Briefly, brain tissues were cut into small pieces and then centrifuged at 13,000*g* for 15 min at 4 °C. Supernatants were collected and concentrations of proteins were determined. Samples were denatured at 95 °C for 5 min and subsequently stored at − 80 °C for further use. Protein samples were loaded onto 10% SDS-PAGE (Bio-Rad, USA) and transferred on PVDF membranes. After being blocked with 5% nonfat dry milk in Tris-buffered saline with 0.1% Tween 20 for 1.5 h, the PVDF membranes were incubated with corresponding primary antibodies overnight at 4 °C. Then, the membranes were incubated with respective HRP-conjugated secondary antibodies for 1 h at room temperature. The membranes were soaked in Super Signal West Pico Chemiluminescent Substrate (Pierce, USA) and then exposed to film (Kodak, USA). The following antibodies were used: anti-AT_1-R (Abcam, ab124505, USA) [27], anti-D3R (Abcam, ab42114, USA) [28], anti-β-actin (Cell Signaling Technology, #4970, USA), and anti-GAPDH (Cell Signaling Technology, #5174, USA).

Quantification of Ang II

The striatum was homogenized in lysis buffer and then centrifuged (13,000*g* for 10 min). The content of Ang II in the striatum supernatant was measured using an enzyme-linked immunosorbent assay (ELISA) kit (USCN Life Science Inc., Wuhan, China) following the manufacturer's instructions.

Immunohistochemistry

Mice were anesthetized with 10% chloralhydrate and perfused with PBS followed by ice-cold 4% paraformaldehyde solution. Brains were fixed overnight in 4% paraformaldehyde solution and then were sliced on a microtome at 10 μm. The brain sections were soaked in 0.2% Triton X-100 in PBS for 30 min, blocked with 10% goat serum in PBS for 1 h, and then incubated with anti-AT_1 antibodies and rabbit anti-TRITC fluorescent-coupled secondary antibodies, respectively. The brain sections were washed with PBS 3 times within 15 min. Nuclei were counterstained with DAPI (2 g/ml) for 10 min.

Cell Culture

SH-SY5Y cell line was purchased from ATCC (American Type Culture Collection, USA). SH-SY5Y cells were cultured in DMEM/F12 supplemented with 10% fetal bovine serum (HyClone, USA), 100 U/ml penicillin, and 100 U/ml streptomycin at 37 °C in a humidity atmosphere of 5% CO_2. Cell counting kit-8 (Beyotime, Shanghai, China) was used to assess cell viability. Briefly, the cell culture media was removed and 100 μl CCK8 media was added to each well in 96-well cell culture plates, then incubated for 0.5~4 h. The optical density was measured at 450 nm using an ELISA plate reader. This procedure was replicated for at least 3 wells.

Statistical Analysis

Statistical significance was measured using an unpaired 2-tailed Student's *t* test when comparing 2 groups. For locomotion

activity data, t test was used to determine significance for 2 groups, and 2-way ANOVAs followed by Bonferroni post-tests were performed with more than 2 groups. One-way ANOVA followed by Tukey's post hoc test was used to determine significance for Western blotting analysis with more than 2 groups. All values included in the figure legends represented mean ± S.D. (*$p < 0.05$, **$p < 0.01$, ***$p < 0.001$; $^{\#}p < 0.05$, $^{\#\#}p < 0.01$, $^{\#\#\#}p < 0.001$). All statistical analyses were performed using the GraphPad Prism 6 software.

Results

AT_1-R Expression Is Upregulated in the Striatum of METH-Treated Mice

As a first step to determine the role of AT_1-R in METH effect, we established a hyperlocomotion model in mice administrated daily with METH (1 mg/kg/day) for 7 days continuously. At the end of the locomotor test, expression of AT_1-R in the PFC, NAc, striatum, and hippocampus were measured by Western blot, respectively. We found that AT_1-R expression was significantly increased in the striatum of mice treated with METH as compared with the saline-treated mice (Fig. 1A, $t_{(4)} = 3.504$, **$p < 0.01$); however, there were no significant changes in the other 3 brain regions. These results showed that upregulation of AT_1-R induced by METH seemed to be brain region specific. As AT_1-R and AT_2-R belong to Ang II receptor types [29], we continued to measure the mRNA expression of both AT_1-R and AT_2-R in the striatum after repeated METH administration. We observed that the mRNA expression of AT_1-R, but not AT_2-R, was significantly increased (Fig. 1B; AT_1-R, $t_{(10)} = 8.047$, ***$p < 0.0001$; AT_2-R, $t_{(10)} = 2.269$, $p > 0.05$). Together, these data showed that repeated METH specifically increased the mRNA and protein expressions of AT_1-R in the striatum. We thus focused on investigating the role of AT_1-R in METH-induced behavior.

To determine the time-dependent expression of AT_1-R responding to METH, we measured AT_1-R expression in the striatum after METH administration for 1, 2, 3, 5, and 7 days, respectively. We observed that there was no change in AT_1-R expression within the first 3 days (Fig. 1C; 1 day, $t_{(6)} = 0.754$, $p > 0.05$; 2 days, $t_{(6)} = 0.267$, $p > 0.05$; 3 days, $t_{(6)} = 2.358$, $p > 0.05$). However, AT_1-R expression was significantly increased after METH treatment for 5 and 7 days, respectively (5 days, $t_{(6)} = 19.596$, ***$p < 0.001$; 7 days, $t_{(6)} = 37.018$, ***$p < 0.001$). These results showed that striatal AT_1-R expression in response to METH seemed to be time-dependent. By using qRT-PCR, we continued to detect the mRNA levels of the 5 members of the DR family as well as dopamine transporter (DAT). Interestingly, we found a significant decrease in D3R expression but an increase in D1R expression in the striatum of METH-treated mice (Fig. 1D; D1R, $t_{(10)} = 4.538$, **$p < 0.01$; D3R, $t_{(6)} = 3.19$, *$p < 0.05$); however, the expressions of D2R, D4R, D5R as well as DAT were not changed. Furthermore, by using Western blot analysis, we also demonstrated that the protein level of D3R was significantly decreased in the striatum after repeat METH administration (Fig. 1E, $t_{(4)} = 2.737$, **$p < 0.01$).

Pharmacological Inhibition of AT_1-R or ACE Attenuates METH-Induced Hyperlocomotion

To further explore the role of brain RAS in METH-induced behavior, we evaluated the effect of 3 small molecular compounds, perindopril (ACE inhibitor), telmisartan (AT_1-R antagonist), and losartan (AT_1-R antagonist), on METH-induced hyperlocomotion, respectively. The former 2 inhibitors can cross the brain–blood barrier (BBB), but the latter cannot [30–32]. METH administration regimen is shown in Fig. 2A. The mice were injected (i.p.) with these inhibitors 30 min before METH injection, respectively. Notably, perindopril significantly reversed METH-induced locomotor activity (Fig. 2B, $F_{(3,\ 344)} = 231.5$, *$p < 0.05$, **$p < 0.01$). We continued to measure Ang II protein expression and found that METH-induced Ang II expression was obviously decreased by perindopril in comparison to the METH alone group (Fig. 2C, $F_{(3,\ 13)} = 36.43$, *$p < 0.05$, ***$p < 0.001$). Meanwhile, we assessed the behavioral effect of losartan and telmisartan on METH-induced hyperlocomotion. Consequently, telmisartan significantly attenuated METH-induced hyperlocomotion (Fig. 2D, $F_{(3,\ 360)} = 493.3$, *$p < 0.05$, **$p < 0.01$), but losartan showed no effect (Fig. 2E). These results showed that inhibition of brain AT_1-R or ACE could inhibit METH behavioral effect. However, losartan, an AT_1-R antagonist but without the capability of crossing the BBB, failed to inhibit METH effect.

Genetic Deletion of AT_1-R Attenuates METH-Induced Hyperlocomotion

We first tested whether the genetic deletion of AT_1-R could influence the basal locomotor activity in wild-type mice. We found that $AT_1^{-/-}$ mice showed no difference of locomotor activity with wild-type mice in the normal condition (data not shown). Interestingly, in comparison to wild-type mice, $AT_1^{-/-}$ mice showed a significantly reduced locomotor activity induced by repeated METH (0.3 and 1 mg/kg, respectively) (Fig. 3A, 0.3 mg/kg METH, day 1, $t_{(16)} = 0.0008$; day 2, $t_{(16)} < 0.0001$; day 3, $t_{(15)} = 0.027$; day 4, $t_{(15)} = 0.014$; day 5, $t_{(16)} = 0.00247$; day 6, $t_{(16)} = 0.0431$; day 7, $t_{(14)} > 0.05$; *$p < 0.05$, **$p < 0.01$, ***$p < 0.001$; Fig. 3B, 1 mg/kg METH, day 1, $t_{(17)} = 0.00319$; day 2, $t_{(18)} = 0.00191$; day 3, $t_{(18)} < 0.0001$; day 4, $t_{(19)} = 0.0007$; day 5, $t_{(18)} < 0.0001$; day 6, $t_{(19)} = 0.00395$; day 7, $t_{(19)} > 0.05$;*$p < 0.05$, **$p < 0.01$, ***$p < 0.001$). However, as compared with the wild-type mice, $AT_1^{-/-}$ mice showed no change in the locomotor activity after

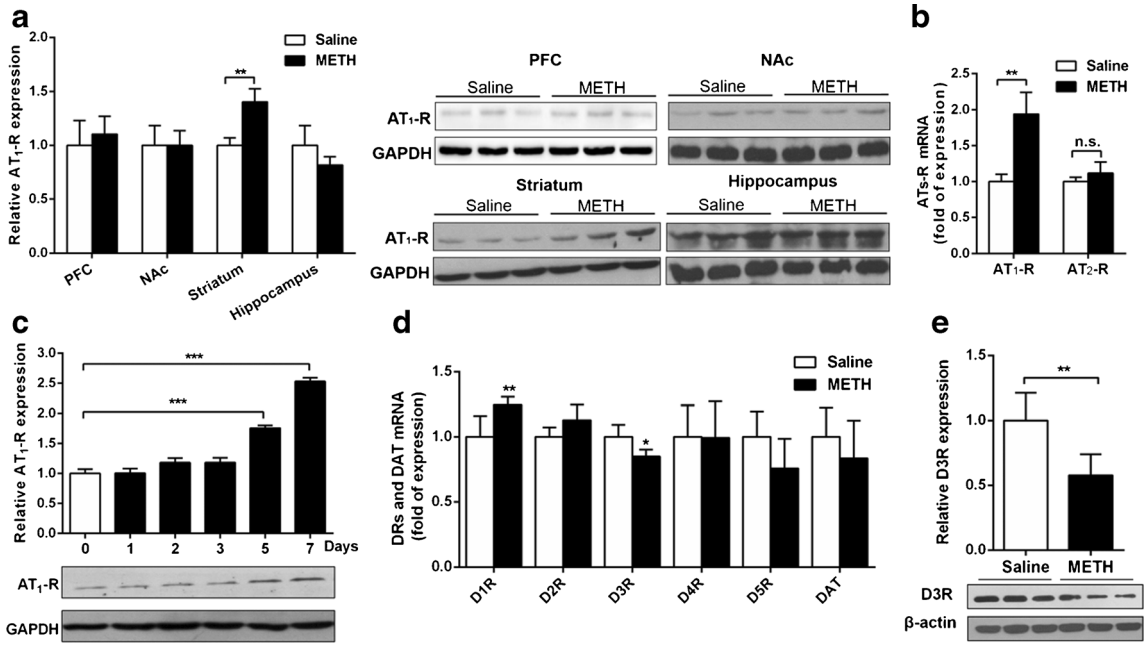

Fig. 1 METH induces upregulation of AT_1-R but downregulation of D3R in the striatum. (**A**) AT_1-R expression was significantly upregulated in the striatum after repeated METH rejections, but not in the PFC, NAc, and hippocampus. $^{**}p < 0.01$, $n = 3$ for each group. (**B**) The mRNA level of AT_1-R, not AT_2-R, was specifically increased in the striatum by repeated METH injection. $n = 6$ for each group. (**C**) Striatal AT_1-R expression at 1, 2, 3, 5, and 7 days after the last injection of METH. $n = 4$ each group. (**D**) The mRNA expression of DRs and DAT was detected after METH administration. $n = 6$ for each group. (**E**) Striatal expression of D3R was downregulated by METH. $n = 3$ for each group. Student's t test, $^{*}p < 0.05$, $^{**}p < 0.01$, $^{***}p < 0.001$

treatment with 3 mg/kg METH (Fig. 3C). Because striatal D3R expression was decreased after repeated METH administration, we then detected the expressions of DRs in $AT_1^{-/-}$ mice. The results showed that the mRNA expressions of D1R, D3R, and D4R were significantly increased in the striatum of $AT_1^{-/-}$ mice as compared with wild-type mice (Fig. 3D, D1R, $t_{(10)} = 2.590$, $^{*}p < 0.05$; D3R, $t_{(9)} = 4.316$, $^{***}p < 0.001$; D4R, $t_{(9)} = 5.095$, $^{***}p < 0.001$). Similarly, Western blotting analysis showed that the expression of D3R was increased significantly in $AT_1^{-/-}$ mice (Fig. 3E, $t_{(4)} = 3.228$, $^{*}p < 0.05$). Interestingly, in comparison to saline group, striatal D3R expression was decreased after repeated METH administration, whereas such effect was significantly attenuated in $AT_1^{-/-}$ mice (Fig. 3F, $F_{(2, 6)} = 3.488$, $^{*}p < 0.05$). These results further indicated that AT_1-R can modulate METH effect and its expression has a negative association with striatal D3R.

Re-Expression of AT_1-R Reverses the Weakened METH Behavioral Effect in $AT_1^{-/-}$ Mice

To further test whether genetic re-expression of AT_1-R could restore the weakened METH effect in $AT_1^{-/-}$ mice, we constructed a lentivirus specifically GFP-tagged AT_1-R (LV-AT_1-GFP) or GFP alone (LV-GFP) (Supplementary Fig. S1). $AT_1^{-/-}$ mice received bilateral intra-striatum injections of vectors expressing either LV-AT_1-GFP or LV-GFP a week before the behavioral test. Compared with $AT_1^{-/-}$ mice treated with LV-GFP, $AT_1^{-/-}$ mice treated with LV-AT_1-GFP showed an increased locomotor activity after repeated METH treatment (Fig. 4A, $F_{(3, 216)} = 159.5$; $^{*}p < 0.05$, $^{**}p < 0.01$; $^{\#}p < 0.05$, $^{\#\#}p < 0.01$). However, under normal condition without METH treatment, $AT_1^{-/-}$ mice receiving intra-striatum injection of LV-AT_1-GFP showed no difference in comparison to the wild-type mice receiving intra-striatum injection of LV-GFP. Collectively, our results suggested that re-expression of AT_1 in the striatum restored the behavioral effect of repeated METH exposure in $AT_1^{-/-}$ mice, demonstrating a role of AT_1-R in mediating METH effect.

Thinking that D3R exhibits an inhibitory effect on motor function [33, 34], we continued to measure striatal D3R expression by Western blotting. Compared with wild-type mice receiving LV-GFP, D3R expression was upregulated in the $AT_1^{-/-}$ mice receiving LV-GFP after repeated METH treatment. Consistently, D3R expression was downregulated in $AT_1^{-/-}$ mice after re-expression of AT_1-R (Fig. 4B, $F_{(3, 12)} = 10.29$, $^{*}p < 0.05$). These results suggested that AT_1-R participates in METH effect possibly through negatively modulating D3R expression.

METH Increases AT_1-R but Reduces D3R Expressions in SH-SY5Y Cells *In Vitro*

By using immunostaining, we observed that AT_1-R was mainly localized in the cytoplasm and membrane of SH-SY5Y cells

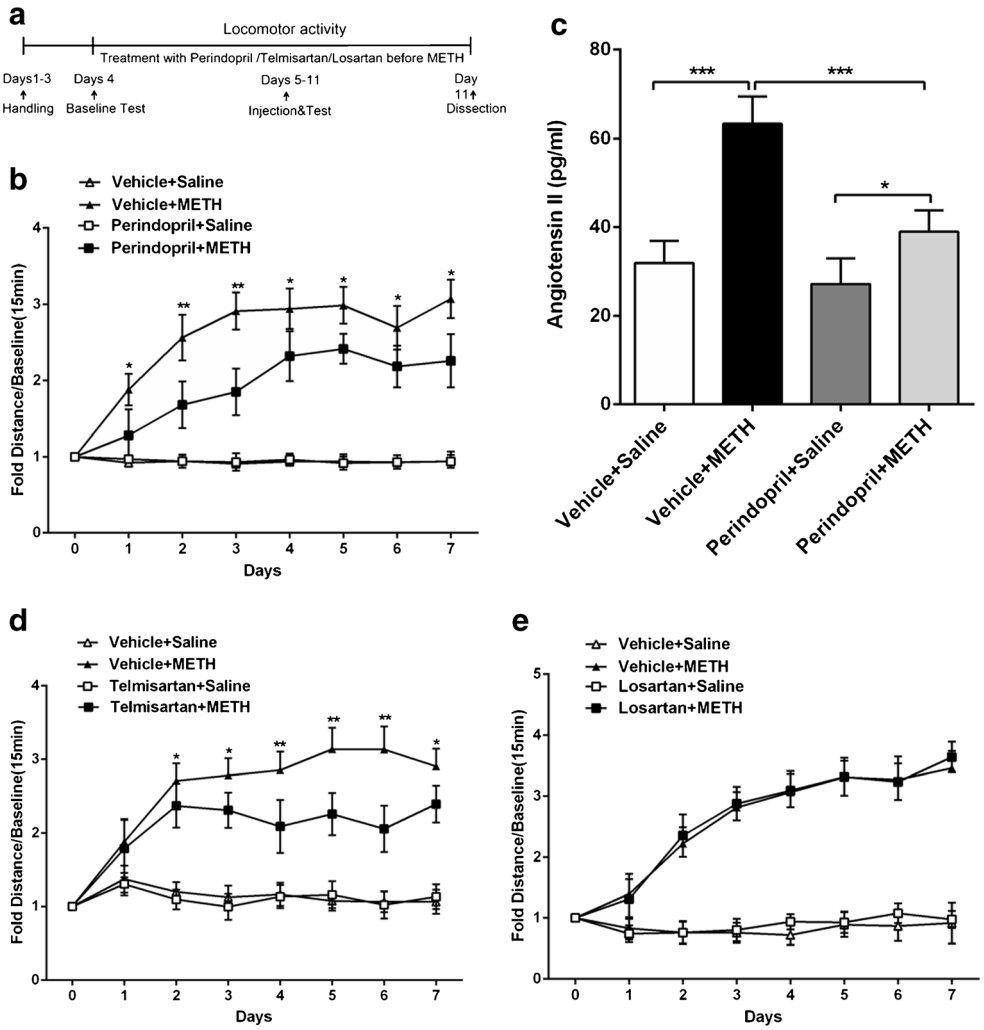

Fig. 2 Pharmacological inhibition of ACE or AT_1-R attenuates METH-induced hyperlocomotion. (**A**) METH induced hyperlocomotion in mice. (**B**) Perindopril, an ACE inhibitor, attenuated METH-induced behavioral sensitization. $*p < 0.05$, $**p < 0.01$, vehicle-saline group $n = 11$, vehicle-METH group $n = 10$, perindopril-METH group $n = 14$, perindopril-saline group $n = 12$. (**C**) Ang II expression, as measured by ELISA, was downregulated by perindopril in METH-treated mice. $*p < 0.05$, $***p < 0.001$, $n = 4$ for each group. (**D**) Telmisartan, an AT_1-R antagonist, attenuated METH-induced hyperlocomotion in mice. $*p < 0.05$, $**p < 0.01$, vehicle-saline group, vehicle-METH group, telmisartan-METH group $n = 12$ for each group, telmisartan-saline group $n = 10$. (**E**) Losartan, an AT_1-R antagonist, showed no effect on METH-induced hyperlocomotion. Vehicle-saline group, $n = 12$; vehicle-METH group, $n = 12$; losartan-METH group, $n = 13$; losartan-saline group, $n = 11$

(Fig. 5A). Through pretest, we observed that the inhibitory concentration (IC_{50}) value of METH for SH-SY5Y cells was approximately 2 mM (exposure for 48 h). We then applied METH at this concentration to perform *in vitro* studies. By using Western blotting, we found that AT_1-R expression was significantly elevated in METH-treated cells, which was in accordance with the aforementioned results *in vivo* (Fig. 5B, $t_{(6)} = 5.073$, $*p < 0.05$). The protein levels of D2R, D4R, and D5R were upregulated after 2 mM METH exposure for 48 h; however, the protein levels of D3R and DAT were downregulated (Fig. 5C, D2R, $t_{(4)} = 5.223$; D3R, $t_{(5)} = 6.452$; D4R, $t_{(3)} = 6.433$; D5R, $t_{(5)} = 4.509$; DAT, $t_{(4)} = 13.631$; $**p < 0.01$, $***p < 0.001$).

Losartan Attenuates METH-Induced Neurotoxicity in SH-SY5Y Cells Possibly Through Downregulating D3R Expression

To investigate whether blocking AT_1-R could attenuate METH-induced cytotoxicity in SH-SY5Y cells, we applied losartan to block AT_1-R *in vitro*. We found that losartan showed no inhibitory effects on SH-SY5Y cells, whereas losartan treatment significantly attenuated METH-induced cytotoxicity in SH-SY5Y cells (Fig. 6A; saline, 1 μM losartan, $t_{(4)} = 5.337$, $*p < 0.05$; saline, 2 μM losartan, $t_{(4)} = 5.255$, $*p < 0.05$; saline, 5 μM losartan, $t_{(4)} = 6.652$, $*p < 0.05$; 2 mM METH, 5 μM losartan, $t_{(4)} = 6.699$, $^{\#\#}p < 0.01$; 2 mM METH, 10 μM losartan, $t_{(4)} = 6.985$, $^{\#\#\#}p < 0.001$). These results suggested that blocking AT_1-R can alleviate METH-induced cytotoxicity. To investigate the association of AT_1-R with DRs, we further measured the mRNA expression levels of DAT and the families of DRs in SH-SY5Y cell after losartan treatment. The results showed that in METH-treated SH-SY5Y cells, the mRNA levels of D1R and D4R were significantly decreased after 10 μM losartan treatment for 48 h, but those of D3R and DAT were significantly increased (Fig. 6B, D1R, $t_{(5)} = 3.761$; D3R, $t_{(10)} = 4.406$; D4R, $t_{(10)} = 4.653$; DAT, $t_{(10)} = 4.777$; $**p < 0.01$, $***p < 0.001$). We continued to verify the change of D3R expression by Western blotting and found that D3R expression was downregulated by METH treatment; however, such effect was reversed by losartan treatment (Fig. 6C,

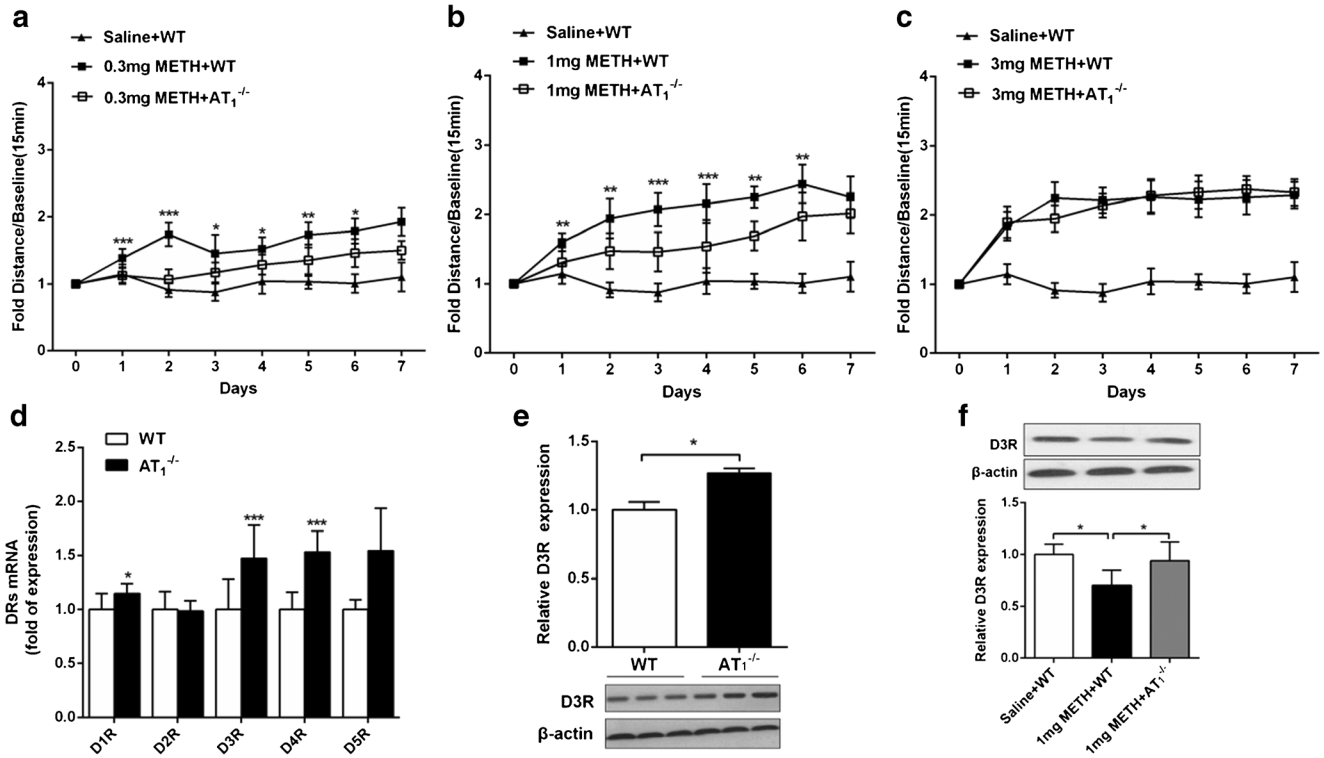

Fig. 3 METH-induced hyperlocomotion is attenuated in $AT_1^{-/-}$ mice. (**A**–**C**) Locomotor activity of wild-type mice or $AT_1^{-/-}$ mice treated with METH (0.3, 1, and 3 mg/kg METH, respectively). $*p < 0.05$, $**p < 0.01$, $***p < 0.001$, $n = 12$ for each group. (**D**) The mRNA expressions of DRs were detected in wild-type and $AT_1^{-/-}$ mice. $*p < 0.05$, $***p < 0.001$, $n = 6$ for each group. (**E**) Protein level of D3R was measured in wild-type and $AT_1^{-/-}$ mice. $*p < 0.05$, $n = 3$ for each group. (**F**) Compared with METH-treated wild-type mice, D3R level was increased by METH in $AT_1^{-/-}$ mice. $*p < 0.05$, $n = 3$ for each group

$F_{(3,\ 12)} = 5.623$, $**p < 0.01$, $***p < 0.001$). Collectively, our results suggested that losartan attenuates METH-induced neurotoxicity of cultured SH-SY5Y cells possibly through downregulating D3R expression.

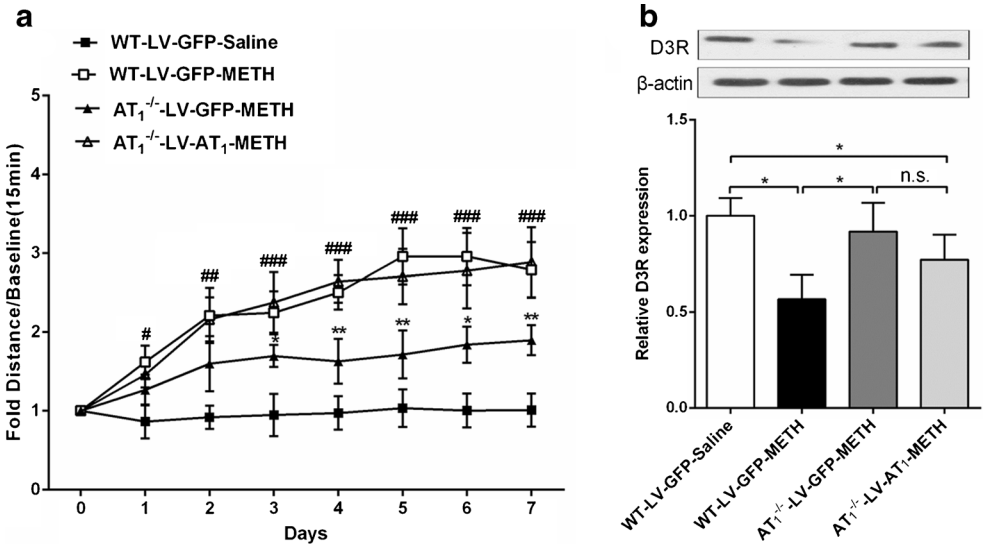

Fig. 4 Intra-striatum re-expression of AT_1 reverses the attenuated behavioral effect of METH in $AT_1^{-/-}$ mice. (**A**) Specific re-expression of AT_1-R by LV-AT_1 in the striatum reversed the attenuated behavioral effect of METH in $AT_1^{-/-}$ mice. *, compared with the $AT_1^{-/-}$-LV-AT_1-METH group, $*p < 0.05$, $**p < 0.01$; #, compared with the WT-LV-GFP-Saline group, $^{\#}p < 0.05$, $^{\#\#}p < 0.01$, $^{\#\#\#}p < 0.001$. $AT_1^{-/-}$-LV-AT_1-METH group $n = 9$; $AT_1^{-/-}$-LV-GFP-METH group $n = 11$; WT-LV-GFP-Saline group $n = 12$; WT-LV-GFP-METH group $n = 12$. (**B**) The D3R protein expression was altered after intra-striatum infusion of LV-AT_1 in $AT_1^{-/-}$ mice. One-way ANOVA followed by Tukey's post-tests was performed, $*p < 0.05$, $n = 4$ for each group

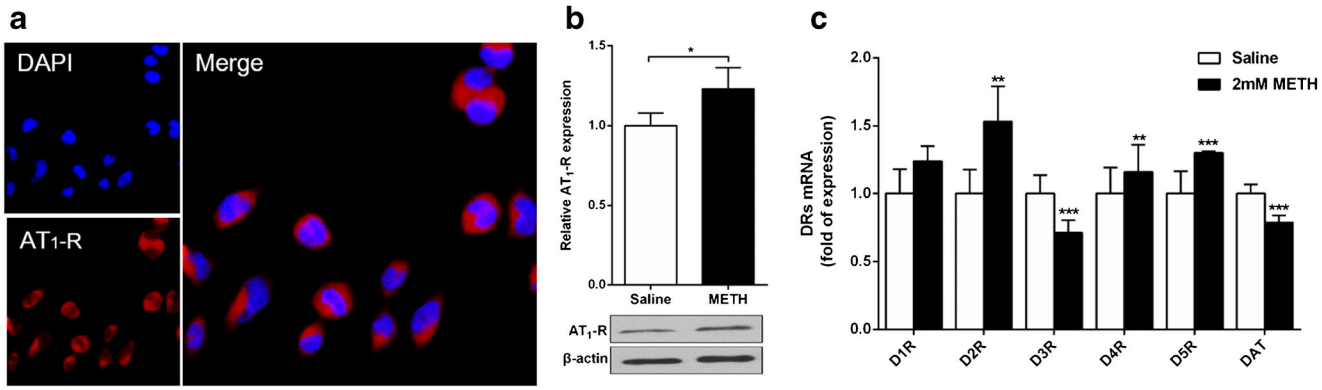

Fig. 5 METH increases AT_1-R but decreases D3R expression in cultured SH-SY5Y cells. (**A**) Representative fluorescence images of SH-SY5Y cells. DAPI (blue), AT_1 (red). (**B**) AT_1-R expression was upregulated in METH-treated cells. $*p < 0.05$, $n = 4$ for each group. (**C**) DRs and DAT mRNA expressions were measured in METH-treated cells. $**p < 0.01$, $***p < 0.001$, $n = 6$ for each group

Discussion

In this study, we demonstrate a modulatory role of Ang II–AT_1-R in METH-induced behavioral effect. The expression of AT_1-R is specifically upregulated in the striatum of METH-treated mice, and the expression of AT_1-R responding to METH displays time dependence. Pharmacological antagonism or genetic deletion of AT_1-R attenuates METH-induced behavioral sensitization, whereas such effect can be reversed by re-expression of AT_1 in the striatum. Striatal AT_1-R expression in METH-treated mice is negatively correlated to D3R expression. Perindopril, a specific ACE inhibitor, significantly attenuates METH-induced hyperlocomotion. Collectively, our findings reveal an unappreciated role of brain RAS in METH effect, which may provide a potential therapeutic target for METH addition.

In fact, the interaction between the dopaminergic system and the RAS has long been discovered by microdialysis studies in brain, which showed that acute Ang II perfusion induces dopamine release, which is blocked by AT_1-R antagonists [16]. Although the involvement of AT_1-R in neuronal activation and AMPH-induced hyperlocomotion has been known [22–24], the role of AT_1-R as well as ACE in METH effect is largely unknown. Pretreatment with AMPH in rats showed an elevated AT_1-R expression both in mRNA and protein levels in the striatum and NAc [24]. This result is partially consistent with our results which showed that repeated METH increased AT_1-R expression in the striatum, but not in NAc. Interestingly, Paz et al. [24] reported that AMPH-induced hyperlocomotion is reversed by losartan administration in the striatum; however, intra-NAc injection of losartan showed no effects. We assume that METH and AMPH may exhibit subtly different effects on the RAS in different brain regions.

As telmisartan, not losartan, can easily pass through the blood–brain barrier and enter the brain [31, 32], it is not surprising that the METH-induced hyperlocomotion was only suppressed by telmisartan in this study. ACE, an angiotensin-converting enzyme, mediates the formation of active octapeptide Ang II. Ang II interacts with its specific

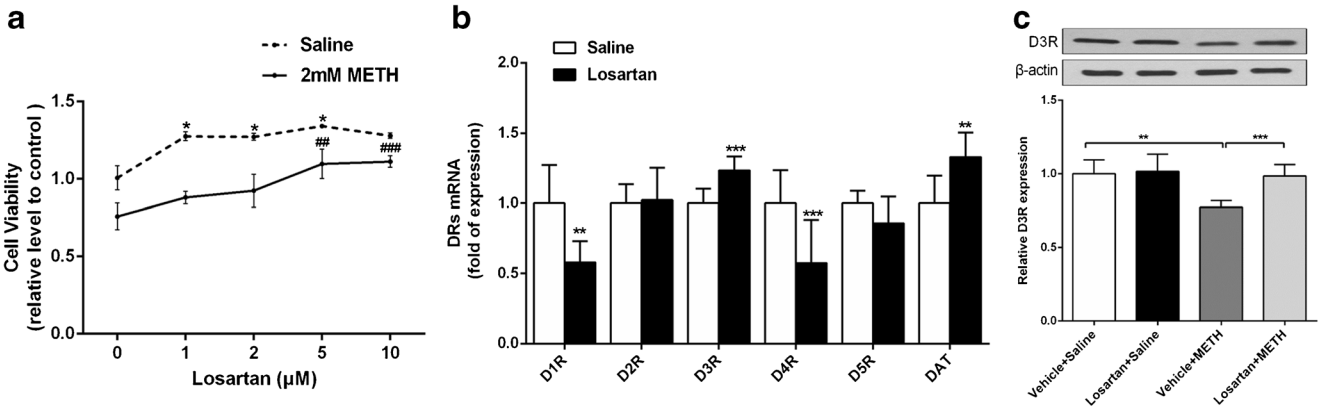

Fig. 6 Losartan attenuates the inhibitory effect of METH on SH-SY5Y cell proliferation accompanied with decreased D3R expression. (**A**) Losartan attenuated the proliferation inhibitory effect of METH on SH-SY5Y cells. $n = 3$ for each group. Saline, $**p < 0.01$; 2 mM METH, $^{\#\#}p < 0.01$, $^{\#\#\#}p < 0.001$. (**B**) The DRs and DAT expressions were measured in SH-SY5Y cells with or without losartan treatment. Student's t test, $**p < 0.01$, $***p < 0.001$, $n = 6$ for each group. (**C**) The decreased D3R level was attenuated by losartan in METH-treated SH-SY5Y cells. One-way ANOVA followed by Tukey's post-tests were performed, $**p < 0.01$, $***p < 0.001$, $n = 4$ for each group

angiotensin receptors (AT_1-R and AT_2-R) and regulates not only blood pressure, cerebral blood flow, and homeostasis-associated behaviors [35–37], but also motor activity, learning, and memory [38, 39]. The ACE inhibitor, perindopril, is able to penetrate the blood–brain barrier and modulate striatal DA synthesis and release [11], and prevents the development of Alzheimer's and Parkinson's disease [40, 41]. Our results unequivocally showed that perindopril decreased the expression of striatal Ang II and attenuated METH-induced hyperlocomotor, suggesting the involvement of ACE and Ang II in the formation of hyperlocomotor induced by METH.

The striatum is strongly related to motivation, movement, self-administration, and behavioral sensitization [42]. Evidence has shown that D3R is mainly expressed in the striatum [43], and has an inhibitory effect on motor function [33, 34]. D3R mutant mice reveal a dramatic potentiation of morphine-induced hyperlocomotion [44]. D3R is necessary for ethanol consumption in mice, and the effect of alcohol intake can be inhibited by D3R gene deletion or selective D3R antagonists [45]. In the present study, repeated METH treatment decreased striatal D3R expression but upregulated AT_1-R expression. Similarly, a previous study revealed an altered interaction between AT_1-R and D3R in the spontaneously hypertensive rats [46]. We further used the mice lacking AT_1-R gene to investigate whether D3R could be a downstream effector of AT_1-R. We found that loss of the AT_1-R significantly elevated striatal D3R expression; on the other hand, genetic intervention by LV-AT_1 re-expression in the striatum of $AT_1^{-/-}$ mice downregulated D3R expression. Therefore, we speculate that the effects of AT_1-R on METH-induced hyperlocomotor may be mediated by the negative regulation of D3R expression. Further study is needed to elucidate the interaction of AT_1-R and D3R and its significance in response to METH.

Previous studies revealed that inhibition of AT_1-R (both pharmacologically and genetically) shows no effect on DA level. Acute administration of AT_1-R antagonists alone does not alter striatal DA level [16, 47] and slightly decreases (~ 15%) DA metabolites [47, 48]. Moreover, chronic administration of AT_1-R antagonist does not alter the levels of DA and its metabolites in the striatum of normal rats [48–50]. However, METH activates neurotransmitter (i.e., dopamine) release by reversing monoamine transport [51]. In this study, we observed that chronic administration of METH induced a decrease in striatal D3 receptor expression, whereas inhibition of AT_1-R (both pharmacologically and genetically) increased the expression of D3 receptor. These changes induced by METH may facilitate striatal dopamine release and motor behavior. Through inhibition of AT_1-R, increased D3 receptor expression may lead to a compensatory decrease in dopamine release [50].

METH-induced neurotoxicity is closely associated with an increased extracellular DA release and subsequent activation of DRs in the dopaminergic system, particularly in the striatum [2]. D1R antagonists systemically co-administered with METH partially protect against METH-induced neurotoxicity [52]. Intra-striatum injection of DR antagonist during METH exposure has also been reported to protect against METH-induced neurotoxicity [53]. Meanwhile, chronic treatment of rats with captopril, an ACE inhibitor, significantly attenuates the loss of nigral DA cell bodies in the progressive MPP+ rat model of parkinsonism, indicating that captopril is neuroprotective for nigrostriatal DA neurons in rodent Parkinson's disease models [54]. Our results also reveal that losartan, a selective AT_1-R antagonist, exerts its neuroprotective effect possibly through modulating D3R expression.

Multiple cellular and molecular mechanisms underlying METH-associated neuronal damage have been proposed, such as increased production of reactive oxygen species, induction of inflammatory responses, and alterations in pro- or anti-apoptotic proteins [55–57]. Ang II and AT_1-R play important roles in neuroinflammation [58, 59], and their interaction activates NADPH-oxidase complex [60], which modulates oxidative stress and neuroinflammatory processes [61, 62]. As AT_1-R and NADPH-oxidase complex are expressed in dopaminergic neurons and glial cells, Ang II may cause neuroinflammation and oxidative stress in dopaminergic neurons through acting on neurons or microglia and stimulate the production of ROS by activation of NAPDH-oxidase [62, 63]. Moreover, AT_1-R overstimulation contributes to neurodegeneration via oxidative damage in Parkinson's disease [64]. A recent study has proved that the effects of METH-induced neuroinflammation and neurotoxicity are attenuated through inhibition of NF-κB/STAT3/ERK and mitochondria-mediated apoptosis pathway in dopaminergic SH-SY5Y cells [65]. A previous study showed that Ang II induces apoptotic death, which is attenuated by pretreatment with Ang II receptor blockers in hippocampal neural stem cells [66]. Evidence has indicated that METH-induced apoptotic death in SH-SY5Y cell line is mediated, at least in part, through an ER-dependent mechanism [67]. Considering these reports together with our findings, we assume that Ang II and AT_1-R may modulate METH-induced neurotoxicity through an immunomodulatory and apoptotic mechanism.

In addition, evidence has shown that AT_1-R and D2R interact directly, forming functional heteromers in the striatal neurons [21]. Our results show that AT_1-R blockade possesses neuroprotective effect against METH-induced neurotoxicity possible via modulating D3R expression. Further research is needed to determine the potential interaction of AT_1-R and D3R as well as its significance in locomotor and neurotoxicity.

In summary, our study reveals that brain RAS mediates METH-induced behavior and neurotoxicity possibly through modulating D3R expression. Blocking AT_1-R could be a potential treatment for METH-induced dependence and neurotoxicity.

Acknowledgments This work was supported by the National Natural Sciences Foundation of China (81571301, 81271467, 81272459, 30970938, 81401105) and National Science & Technology Major Project (2018ZX09201017) .

Required Author Forms Disclosure forms provided by the authors are available with the online version of this article.

Author Contributions X.B.C, L.H.J, and R.M.Z conceived and designed the experiments. L.H.J and R.M.Z performed the experiments and analyzed the data. Y.L, X.S, D.Q.F, H.G, L.L, H.L.L, and Y.L.Z contributed reagents, materials, and/or analysis tools. X.B.C, L.H.J, R.M.Z, and Q.B wrote the main manuscript text. All authors read and approved the final manuscript.

Compliance with Ethical Standards

Disclosures The authors declare no competing financial interests.

References

1. Mattson M E. Emergency department visits involving methamphetamine: 2007 to 2011. The CBHSQ Report. Rockville (MD)2013.
2. Moratalla R, Khairnar A, Simola N, et al. Amphetamine-related drugs neurotoxicity in humans and in experimental animals: main mechanisms. Prog Neurobiol. 2017;155:149–170.
3. Bernheim A, See R E, Reichel C M. Chronic methamphetamine self-administration disrupts cortical control of cognition. Neurosci Biobehav R. 2016;69:36–48.
4. Heidbreder C A, Newman A H. Current perspectives on selective dopamine D3 receptor antagonists as pharmacotherapeutics for addictions and related disorders. Ann N Y Acad Sci. 2010;1187:4–34.
5. B Le Foll J-C S, P Sokoloff. Disruption of nicotine conditioning by dopamine D3 receptor ligands. Mol Psychiatry 2003;8:225–s30.
6. Vorel S R, Ashby C R, Jr., Paul M, et al. Dopamine D3 receptor antagonism inhibits cocaine-seeking and cocaine-enhanced brain reward in rats. J Neurosci. 2002;22:9595–9603.
7. Xi Z X, Newman A H, Gilbert J G, et al. The novel dopamine D3 receptor antagonist NGB 2904 inhibits cocaine's rewarding effects and cocaine-induced reinstatement of drug-seeking behavior in rats. Neuropsychopharmacol. 2006;31:1393–1405.
8. Wolf M E. Synaptic mechanisms underlying persistent cocaine craving. Nat Rev Neurosci. 2016;17:351–365.
9. Lee B, London E D, Poldrack R A, et al. Striatal dopamine d2/d3 receptor availability is reduced in methamphetamine dependence and is linked to impulsivity. J Neurosci. 2009;29:14734–14740.
10. Kohno M, Okita K, Morales A M, et al. Midbrain functional connectivity and ventral striatal dopamine D2-type receptors: link to impulsivity in methamphetamine users. Mol Psychiatry. 2016;21:1554–1560.
11. Rodriguez-Perez A I, Valenzuela R, Villar-Cheda B, Guerra M J, Labandeira-Garcia J L. Dopaminergic neuroprotection of hormonal replacement therapy in young and aged menopausal rats: role of the brain angiotensin system. Brain. 2012;135:124–138.
12. Barnes D E, Yaffe K. The projected effect of risk factor reduction on Alzheimer's disease prevalence. Lancet Neurol. 2011;10:819–828.
13. Wright J W, Kawas L H, Harding J W. The development of small molecule angiotensin IV analogs to treat Alzheimer's and Parkinson's diseases. Prog Neurobiol. 2015;125:26–46.
14. Staff P M. Correction: cardiovascular and renal outcomes of renin-angiotensin system blockade in adult patients with diabetes mellitus: a systematic review with network meta-analyses. PLoS Med. 2016;13:e1002064.
15. Saavedra J M, Ando H, Armando I, et al. Anti-stress and anti-anxiety effects of centrally acting angiotensin II AT1 receptor antagonists. Regul Pept. 2005;128:227–238.
16. Brown D C, Steward L J, Ge J, Barnes N M. Ability of angiotensin II to modulate striatal dopamine release via the AT1 receptor in vitro and in vivo. Br J Pharmacol. 1996;118:414–420.
17. Diaz-Ruiz C, Rodriguez-Perez A I, Beiroa D, Rodriguez-Pallares J, Labandeira-Garcia J L. Reciprocal regulation between sirtuin-1 and angiotensin-II in the substantia nigra: implications for aging and neurodegeneration. Oncotarget. 2015;6:26675–26689.
18. Saavedra J M. Beneficial effects of angiotensin II receptor blockers in brain disorders. Pharmacol Res. 2017:91–103.
19. Narayanaswami V, Somkuwar S S, Horton D B, Cassis L A, Dwoskin L P. Angiotensin AT1 and AT2 receptor antagonists modulate nicotine-evoked [(3)H]dopamine and [(3)H]norepinephrine release. Biochem Pharmacol. 2013;86:656–665.
20. Li D, Scott L, Crambert S, et al. Binding of losartan to angiotensin AT1 receptors increases dopamine D1 receptor activation. J Am Soc Nephrol. 2012;23:421–428.
21. Martinez-Pinilla E, Rodriguez-Perez A I, Navarro G, et al. Dopamine D2 and angiotensin II type 1 receptors form functional heteromers in rat striatum. Biochem Pharmacol. 2015;96:131–142.
22. Paz M C, Marchese N A, Cancela L M, Bregonzio C. Angiotensin II AT(1) receptors are involved in neuronal activation induced by amphetamine in a two-injection protocol. Biomed Res Int. 2013;2013:534817.
23. Paz M C, Assis M A, Cabrera R J, Cancela L M, Bregonzio C. The AT(1) angiotensin II receptor blockade attenuates the development of amphetamine-induced behavioral sensitization in a two-injection protocol. Synapse. 2011;65:505–512.
24. Paz M C, Marchese N A, Stroppa M M, et al. Involvement of the brain renin-angiotensin system (RAS) in the neuroadaptive responses induced by amphetamine in a two-injection protocol. Behav Brain Res. 2014;272:314–323.
25. Casarsa B S, Marinzalda M A, Marchese N A, et al. A previous history of repeated amphetamine exposure modifies brain angiotensin II AT1 receptor functionality. Neuroscience. 2015;307:1–13.
26. Li Y, Zhu R, Wang W, et al. Arginine methyltransferase 1 in the nucleus accumbens regulates behavioral effects of cocaine. J Neurosci. 2015;35:12890–12902.
27. Czikora I, Feher A, Lucas R, Fulton D J, Bagi Z. Caveolin-1 prevents sustained angiotensin II-induced resistance artery constriction and obesity-induced high blood pressure. Am J Physiol Heart Circ Physiol. 2015;308:H376–H385.
28. Li Y, Kuzhikandathil E V. Molecular characterization of individual D3 dopamine receptor-expressing cells isolated from multiple brain regions of a novel mouse model. Brain Struct Funct. 2012;217:809–833.
29. Oliveira L, Costa-Neto C M, Nakaie C R, et al. The angiotensin II AT1 receptor structure-activity correlations in the light of rhodopsin structure. Physiol Rev. 2007;87:565–592.
30. Dagenais G R, Pogue J, Fox K, Simoons M L, Yusuf S. Angiotensin-converting-enzyme inhibitors in stable vascular disease without left ventricular systolic dysfunction or heart failure: a combined analysis of three trials. Lancet. 2006;368:581–588.
31. Habashi J P, Judge D P, Holm T M, et al. Losartan, an AT1 antagonist, prevents aortic aneurysm in a mouse model of Marfan syndrome. Science. 2006;312:117–121.
32. Fichet J, Bressolle C. Telmisartan for prevention of cardiovascular events. New Engl J Med. 2009;360:302–303.
33. Orio L, Wee S, Newman A H, Pulvirenti L, Koob G F. The dopamine D3 receptor partial agonist CJB090 and antagonist PG01037 decrease progressive ratio responding for methamphetamine in rats with extended-access. Addict Biol. 2010;15:312.

34. Spiller K, Xi Z-X, Peng X-Q, et al. The selective dopamine D3 receptor antagonists SB-277011A and NGB 2904 and the putative partial D3 receptor agonist BP-897 attenuate methamphetamine-enhanced brain stimulation reward in rats. Psychopharmacology. 2008;196:533–542.
35. Zhang H, Han G W, Batyuk A, et al. Structural basis for selectivity and diversity in angiotensin II receptors. Nature. 2017. 544(7650): 327–332.
36. John W. Wright, Joseph W. Harding. Brain renin-angiotensin—a new look at an old system. Prog Neurobiol. 2011;95:49–67.
37. Feng Y Y X, Xia H, Bindom SM, et al. Angiotensin-converting enzyme 2 overexpression in the subfornical organ prevents the angiotensin II-mediated pressor and drinking responses and is associated with angiotensin II type 1 receptor downregulation. Circ Res. 2008;102:729–736.
38. Wright J W, Harding J W. The brain angiotensin system and extracellular matrix molecules in neural plasticity, learning, and memory. Prog Neurobiol. 2004;72:263–293.
39. De Bundel D, Smolders I, Vanderheyden P, Michotte Y. Ang II and Ang IV: unraveling the mechanism of action on synaptic plasticity, memory, and epilepsy. CNS Neurosci Ther. 2008;14:315–339
40. Kehoe PG W S, Al Mulhim N, Palmer LE, Miners JS. Angiotensin-converting enzyme 2 is reduced in Alzheimer's disease in association with increasing amyloid-β and tau pathology. Alzheimers Res Ther. 2016;8:50.
41. Kaur P M A, Kaur M. The implications of angiotensin-converting enzymes and their modulators in neurodegenerative disorders: current and future perspectives. ACS Chem Neurosci. 2015;6:508–521.
42. Volkow N D, Morales M. The brain on drugs: from reward to addiction. Cell. 2015;162:712–725.
43. Fiorentini C, Busi C, Spano P, Missale C. Dimerization of dopamine D1 and D3 receptors in the regulation of striatal function. Curr Opin Pharmacol. 2010;10:87–92.
44. Narita M, Mizuo K, Mizoguchi H, et al. Molecular evidence for the functional role of dopamine D3 receptor in the morphine-induced rewarding effect and hyperlocomotion. J Neurosci. 2003;23:1006–1012.
45. Leggio G M, Camillieri G, Platania C B M, et al. Dopamine D3 receptor is necessary for ethanol consumption: an approach with buspirone. Neuropsychopharmacol. 2014;39:2017–2028.
46. Zeng C, Asico L D, Wang X, et al. Angiotensin II regulation of AT1 and D3 dopamine receptors in renal proximal tubule cells of SHR. Hypertension. 2003;41:724–729.
47. Jenkins T A. Effect of angiotensin-related antihypertensives on brain neurotransmitter levels in rats. Neurosci Lett. 2008;444: 186–189.
48. Mendelsohn F A, Jenkins T A, Berkovic S F. Effects of angiotensin II on dopamine and serotonin turnover in the striatum of conscious rats. Brain Res. 1993;613:221–229.
49. Dwoskin L P, Jewell A L, Cassis L A. DuP 753, a nonpeptide angiotensin II-1 receptor antagonist, alters dopaminergic function in rat striatum. Naunyn Schmiedebergs Arch Pharmacol. 1992;345: 153–159.
50. Dominguez-Meijide A, Villar-Cheda B, Garrido-Gil P, et al. Effect of chronic treatment with angiotensin type 1 receptor antagonists on striatal dopamine levels in normal rats and in a rat model of Parkinson's disease treated with L-DOPA. Neuropharmacology. 2014;76:156–168.
51. Howell L L, Kimmel H L. Monoamine transporters and psychostimulant addiction. Biochem Pharmacol. 2008;75: 196–217.
52. Broening H W, Morford L L, Vorhees C V. Interactions of dopamine D1 and D2 receptor antagonists with D-methamphetamine-induced hyperthermia and striatal dopamine and serotonin reductions. Synapse. 2005;56:84–93.
53. Gross N B, Duncker P C, Marshall J F. Striatal dopamine D1 and D2 receptors: widespread influences on methamphetamine-induced dopamine and serotonin neurotoxicity. Synapse. 2011;65:1144–1155.
54. Sonsalla P K, Coleman C, Wong L Y, et al. The angiotensin converting enzyme inhibitor captopril protects nigrostriatal dopamine neurons in animal models of parkinsonism. Exp Neurol. 2013;250:376–383.
55. Coelho-Santos V, Goncalves J, Fontes-Ribeiro C, Silva A P. Prevention of methamphetamine-induced microglial cell death by TNF-alpha and IL-6 through activation of the JAK-STAT pathway. J Neuroinflamm. 2012;9:103.
56. Kanthasamy K, Gordon R, Jin H, et al. Neuroprotective effect of resveratrol against methamphetamine-induced dopaminergic apoptotic cell death in a cell culture model of neurotoxicity. Curr Neuropharmacol. 2011;9:49–53.
57. Berman S B, Zigmond M J, Hastings T G. Modification of dopamine transporter function: effect of reactive oxygen species and dopamine. J Neurochem. 1996;67:593–600.
58. Rodriguez-Perez AI B A, Diaz-Ruiz C, Garrido-Gil P, Labandeira-Garcia JL. Crosstalk between insulin-like growth factor-1 and angiotensin-II in dopaminergic neurons and glial cells: role in neuroinflammation and aging. Oncotarget. 2016;7:30049–30067.
59. Dominguez-Meijide A, Rodriguez-Perez A I, Diaz-Ruiz C, Guerra M J, Labandeira-Garcia J L. Dopamine modulates astroglial and microglial activity via glial renin-angiotensin system in cultures. Brain Behav Immun. 2017;62:277–290.
60. Hoogwerf B J. Renin-angiotensin system blockade and cardiovascular and renal protection. Am J Cardiol. 2010;105:30A-305A.
61. Labandeira-Garcia J L, Rodriguez-Pallares J, Rodriguez-Perez A I, et al. Brain angiotensin and dopaminergic degeneration: relevance to Parkinson's disease. Am J Neurodegener Dis. 2012;1:226–244.
62. Munoz A, Rey P, Guerra M J, et al. Reduction of dopaminergic degeneration and oxidative stress by inhibition of angiotensin converting enzyme in a MPTP model of parkinsonism. Neuropharmacology. 2006;51:112–120.
63. Qin L, Liu Y, Wang T, et al. NADPH oxidase mediates lipopolysaccharide-induced neurotoxicity and proinflammatory gene expression in activated microglia. J Biol Chem. 2004;279: 1415–1421.
64. Rey P, Lopez-Real A, Sanchez-Iglesias S, et al. Angiotensin type-1-receptor antagonists reduce 6-hydroxydopamine toxicity for dopaminergic neurons. Neurobiol Aging. 2007;28:555–567.
65. Park J-H, Seo Y H, Jang J-H, et al. Asiatic acid attenuates methamphetamine- induced neuroinflammation and neurotoxicity through blocking of NF-kB/ STAT3/ERK and mitochondria-mediated apoptosis pathway. J Neuroinflamm. 2017;14:240.
66. Kim M-S, Lee G-H, Kim Y-M, et al. Angiotensin II causes apoptosis of adult hippocampal neural stem cells and memory impairment through the action on AMPK-PGC1a signaling in heart failure. Stem Cells Transl Med. 2017;6:1491–1503.
67. Wongprayoon P, Govitrapong P. Melatonin protects SH-SY5Y neuronal cells against methamphetamine-induced endoplasmic reticulum stress and apoptotic cell death. Neurotox Res. 2017;31:1–10.